PORTIONS OF THIS DOCUMENT ARE ILLEGIBLE

DOE/ER/01383-415G
TUNL-PUB-115-87

GIANT RESONANCE EFFECTS IN RADIATIVE CAPTURE

KURT A. SNOVER,
Department of Physics, University of Washington,
Seattle, WA 98195

I. INTRODUCTION

I've been asked to describe the technique of capture reaction studies of giant resonance properties. Most of my discussion will be based on examples, since the clearest way to illustrate technique is by example, and I have tried to choose recent measurements of general interest. In addition, since one's understanding of the physics of giant resonance properties is best achieved by comparing results of quite different types of experiments, I have included such comparisons where appropriate. Since this paper is not meant to be a review, I've not attempted to adequately represent all of the recent work of interest in this field; indeed, this would be impossible in such a short space. Most of the recent work of interest has been in proton capture, in part because of the great utility (and availability) of polarized beams, and most of my discussion will be about this reaction. I'll also briefly discuss alpha capture, which has been a useful tool for exploring isoscalar (IS) E2 strength, and neutron capture, which is coming of age with the high quality work being done now at TUNL.

First, I'd like to mention some advantages of capture reactions:

a) Detailed information with good energy resolution can be obtained on the contributions of different multipolarities to a specific reaction channel. The α, $\vec{p}$ and $\vec{n}$ entrance channels allow the least ambiguous separation of different multipoles for reactions with simple spin sequences. Radiative capture has also been observed with d, ^{3}He, ^{7}Li and ^{12}C projectiles. The sensitivity of capture to E1, M1, E2 and E3 multipoles has been demonstrated: this relatively restricted sensitivity to low order multipoles is a simplifying advantage.

b) Because different multiples interfere in the differen-

tial cross section, one has an enhanced sensitivity to relatively weak multipoles. Thus information about the phases and the magnitudes of reaction amplitudes is obtained.

c) Specific information may be obtained on the isospin character (isoscalar vs. isovector) of the radiation and on isospin purity.

II. METHOD OF ANALYSIS FOR NUCLEON CAPTURE

The cross section $\sigma(E,\theta)$ and analyzing power $A(E,\theta)$ for the capture of polarized particles may be defined in the usual manner as

$$\sigma(E,\theta) = [\sigma\uparrow(E,\theta) + \sigma\downarrow(E,\theta)]/2 \tag{1}$$

and

$$\sigma(E,\theta)A(E,\theta) = [\sigma\uparrow(E,\theta) - \sigma\downarrow(E,\theta)]/2P \tag{2}$$

where $\sigma\uparrow$ and $\sigma\downarrow$ are the cross sections for an incident beam of energy E and vector polarization of magnitude P oriented along ($\uparrow$) or againt ($\downarrow$) the normal $\hat{n} = \vec{K}_{in} \times \vec{K}_{out}$ to the reaction plane.

The dependence on γ-ray emission angle θ may be expanded as

$$\sigma(E,\theta) = \sum_{K=0}^{2L_{max}} A_K(E)Q_K P_K(\cos\theta) \tag{3}$$

and

$$\sigma(E,\theta)A(E,\theta) = \sum_{K=1}^{2L_{max}} B_K(E)Q_K P_K^1(\cos\theta) \tag{4}$$

Here $\sigma_{total} = 4\pi A_o$, L_{max} is the maximum multipole which contributes ($L_{max} = 2$ for dipole + quadrupole) and the Q_K are the usual angular attenuation factors. It is often convenient to define fractional Legendre coefficients $a_K = A_K/A_o$, $b_K = B_K/A_o$. For the capture of polarized spin-1/2 particles on unpolarized targets, with only the γ-ray intensity (at a given energy and angle) observed in the outgoing channel, the above equations completely specify the (parity-allowed)capture process.

The usual angular momentum coupling rules tell us that interference between opposite (same) parity radiations contributes to the odd (even) coefficients so that E1-M1 interference contributes to A_1 and B_1, E1-E2 to A_1, B_1, A_3, B_3, etc. The exact relations may be written down as

$$A_k = \sum_{tt'} D_{tt'k} \, \mathrm{Re}\, T_t \, T^*_{t'} \qquad (5)$$

and

$$B_k = \sum_{tt'} f_k(tt') D_{tt'k} \, \mathrm{Im}\, T_t \, T^*_{t'} \qquad (6)$$

where T_t, $T_{t'}$ are the reaction amplitudes for different channels t and t', the $D_{tt'k}$ are angular momentum coupling factors and

$$f_k(tt') = [j'(j'+1) + \ell(\ell+1) - j(j+1) - \ell'(\ell'+1)]/2k(k+1) \qquad (7)$$

where ℓ, j, ℓ', j' are the interfering orbital and total angular momenta for the incident nucleon.

For the simplest spin sequences ($J_{target} = 1/2$, $J_{residual} = 0$ or vice versa), only 2 complex reaction amplitudes contribute for each multipole. For cases of this sort involving $1p_{1/2}$-shell targets, the amplitudes are

$$\text{E1} : s_{1/2}e^{i\phi_{s1/2}}, \; d_{3/2}e^{i\phi_{d3/2}}$$

$$\text{E2} : p_{3/2}e^{i\phi_{p3/2}}, \; f_{5/2}e^{i\phi_{f5/2}}$$

$$\text{M1} : p_{1/2}e^{i\phi_{p1/2}}, \; p'_{3/2}e^{i\phi'_{p3/2}}$$

If only electric multipoles contribute at a given energy, the problem is overdetermined (e.g., 9 independent A_K, B_K versus 7 amplitude parameters for E1 + E2) whereas if magnetic multipoles contribute, the problem is underdetermined (E1 + E2 + M1 requires 11 amplitude parameters) and this latter situation represents a limitation to the technique. However, as we show below, one may use $(\vec{p},\gamma)$ to uniquely determine E1 amplitudes, identify the multipolarity E1, E2 or M1 of resonances, and provide interesting limits on E2 cross sections for broadly distributed strength in the continuum.

III. E1 PROPERTIES IN $(\vec{p},\gamma)$

At most bombarding energies E1 is the dominant multipole in (p,γ) and measurements with polarized beam place important restrictions on the E1 amplitudes and phases which contribute to the capture process. The pioneering work of this sort, including $(\vec{p},\gamma)$ measurements of E2 strength, was carried out at Stanford University.[1,2] For the simple spin sequences described above, where only 2 complex E1 amplitudes may con-

tribute, $(\vec{p},\gamma)$ angular distribution measurements restrict the amplitudes to 2 possible solutions. This 2-fold ambiguity is inherent, resulting from the quadratic nature of the equations relating the amplitudes to the data. A typical example in light nuclei is the $^{12}C(p,\gamma_0)^{13}N$ reaction,[3,4] illustrated in Fig. 1. The GDR region extends from $E_p \sim 8$-30 MeV with $(\vec{p},\gamma_0)$ angular distribution results available[3] for E_p = 10-17 MeV. Only incoming s- and d-wave amplitudes (with j = 1/2 and 3/2, respectively) may contribute to E1 capture, and Fig. 1 shows that one of the 2 solutions is predominantly d-wave ($d_>$) and the other predominantly s-wave ($s_>$). Similar $d_>$ and $s_>$ solutions are obtained for other capture reactions such as $^{14}C(\vec{p},\gamma_0)^{5}$ and $^{15}N(\vec{p},\gamma_0)^{2,6,7}$ (see Fig. 2), indicating that one is observing a general feature

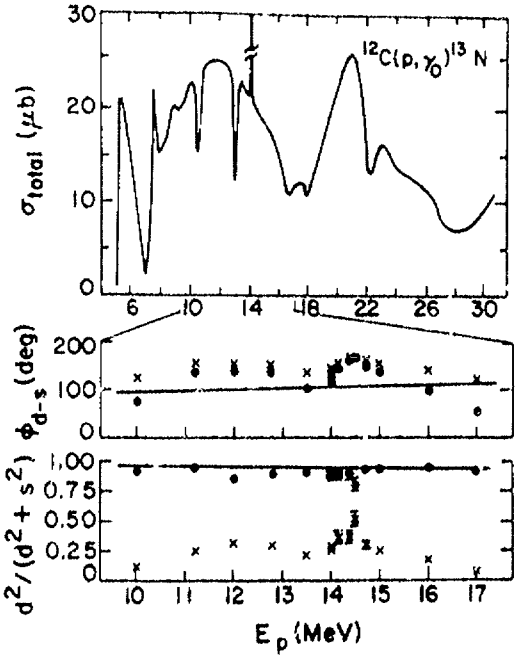

Figure 1. Upper part: σ_{total} for $^{12}C(\vec{p},\gamma_0)$ (refs. 3,4). Lower part: The d-s phase difference and the relative d-wave intensity for Ep = 10-17 MeV (ref. 3 plus ref. 5 for $14 < E_p < 15$ MeV). The points and crosses correspond to the $d_>$ and $s_>$ solutions, respectively. The solid lines are DSD calculations described in ref. 3.

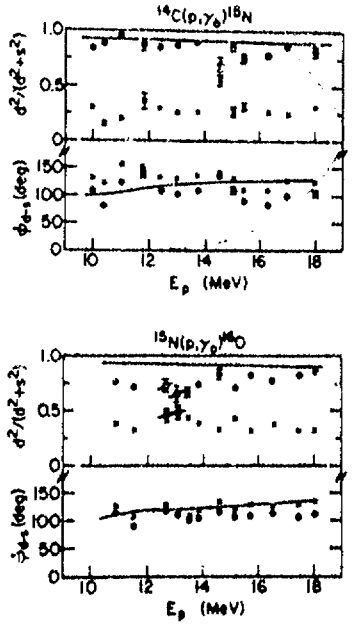

Figure 2. The relative d-wave intensity and the d-s phase difference for $^{14}C(\vec{p},\gamma_0)$ (ref. 5) and $^{15}N(\vec{p},\gamma_0)$ (ref. 6,7). The solid curves are DSD model predictions (see ref. 7).

of the GDR build on $1p_{1/2}$-shell nuclei. The $d_>$ solution is expected on theoretical grounds—virtually all models of radiative capture through the GDR such as the doorway-state[8] or the direct-semidirect (DSD)[7] models predict that d-waves should dominate, with results in reasonable agreement with the experimental data if the $d_>$ solution is the correct (physical) one.

The expectation that d-waves should dominate stems from basic shell model considerations. As discussed by Wilkinson many years ago,[9] the GDR should be dominated by nucleon excitations of the form $n\ell \rightarrow n'\ell'$ where $n\ell$ is an occupied shell model orbital and $n'\ell'$ an unoccupied orbital, with $n' = n$ and $\ell' = \ell + 1$. Consequently, when the target nucleus is related to the final nucleus by removal of a nucleon from orbital n, radiative capture amplitudes with $\ell' = \ell + 1$ should dominate in the GDR region. In the 1p-shell this means d-wave nucleon emission from the GDR should dominate.

Thus this basic shell model property of the GDR could be tested if one could determine uniquely the E1 amplitudes in radiative capture; i.e., determine if the $d_>$ solution is the physically correct one. At Seattle we did this recently[10] in the $^{12}C(\vec{p},\gamma_0)$ reaction by studying the interference between the lowest T = 3/2 M1(E2) resonance at E_p = 14.23 MeV and the E1 background. The basic idea is to use interference with a known resonance to determine unknown properties of the background.

The dominant M1-E1 interference effects should appear in the A_1 and B_1 coefficients; hence we measured excitation curves at 90° with a polarized beam and 55° and 125° with an unpolarized beam. The results are shown in Fig. 3 for

$$[\sigma(55°) + \sigma(125°)]/2 = A_0 - 0.39\ A_4 \propto \sigma_{total}/4\pi$$

$$\sigma A(90°) = B_1 - 1.53\ B_3$$

$$[\sigma(55°) - \sigma(125°)]/2 = 0.57\ A_1 - 0.39\ A_3 \quad .$$

The experimental data for the latter 2 quantities clearly show pronounced interference effects.

In our calculations we used the T = 3/2 resonance parameters of ref. 11 and background E1 and E2 amplitudes determined from off-resonance angular distributions. The shapes of $\sigma(90°)$ (not shown) and $\sigma(55°) + \sigma(125°)$ were used to determine the asymmetric energy resolution and the resonance energy. $\sigma A(90°)$ was then fitted with the phase of the M1 resonance relative to the E1 background as the only free parameter. The 2 bands (Fig. 3) indicate the range of $d_>$ and $s_>$ solutions obtained from off-resonance angular distributions at E_p = 14.00, 14.17, 14.39 and 14.49 MeV. The

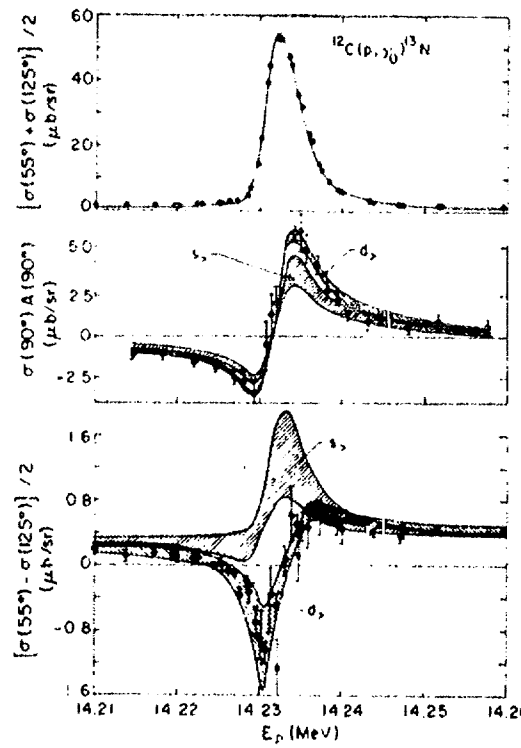

Figure 3. Excitation curves taken near the lowest T = 3/2 resonance in $^{12}C(p,\gamma_0)^{13}N$ (ref. 10). The solid curve in the top part is a calculated fit. The bands in the lower 2 parts represent the spread of calculated curves for the $d_>$ and $s_>$ solutions consistent with off-resonance angular distributions.

corresponding bands for the 55-125° cross section difference were calculated with no free parameters. These bands are insensitive to the E2 parameters, which serve only to determine the off-resonance values for $\sigma A(90°)$ and $\sigma(55°) - \sigma(125°)$. The results clearly select the $d_>$ solution as the physically correct one.

As well as the gross structure, the fine structure of E1 amplitudes has an important bearing on the character of the GDR—see, for example, the discussion of ref. 12 regarding secondary doorway states in the ^{16}O GDR.

IV. E2 STRENGTH IN (p,γ_0)

Here one should distinguish roughly 3 different energy regimes in light nuclei: (1) The low energy ($E_p \lesssim 10$ MeV) region of semi-isolated resonances where, in many cases, the multipolarities of individual resonances may be determined

uniquely. This is generally the region below the main giant electric resonances, where one may explore low-energy fragments. (2) The GDR region ($E_p \sim$ 10-20 MeV). Here resonances are broad and one tries at a given energy to decompose the continuum into its multipole constituents. (3) Above the GDR ($E_p \gtrsim$ 20 MeV) where no polarized beam data are available. and higher multipoles like E3 may be important.

By far the most extensive $(\vec{p},\gamma_0)$ data exist for the GDR region for $A \lesssim 20$. The results for E2 cross sections fall into 2 categories: a) cases where one does not see strong deviations from direct E2 capture predictions, including $^{12}C(\vec{p},\gamma_0)$ (E_p = 10-17 MeV),[3] $C^{13}(\vec{p},\gamma_1)$ (8-16 MeV),[13] and $^{14}C(\vec{p},\gamma_0)$ (10-18 MeV)[5]; and b) other cases where a significant E2 contribution in excess of direct capture may be present, such as $^{14}N(\vec{p},\gamma_0)$ (see below) and perhaps $^{11}B(\vec{p},\gamma_0)$ (ref. 14).

This is illustrated in the case of $^{12}C(\vec{p},\gamma_0)^{13}N$ in Figs. 4 and 5. Figure 5 shows the E2 cross sections deduced from the measured a_i, b_i coefficients displayed in Fig. 4. The E2 cross sections are extracted by solving equations (5) and (6) for the T-matrix amplitudes and phases assuming only E1 and E2 radiation and then calculating $\sigma_{E2} = p^2 + f^2$.

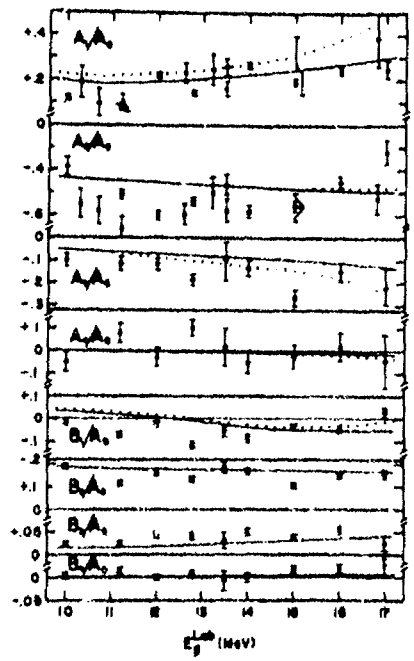

Figure 4. $^{12}C(\vec{p},\gamma_0)$ angular distribution coefficients (ref. 3). The solid curve is a DSD model calculation with direct E2 and the dashed curve includes collective E2.

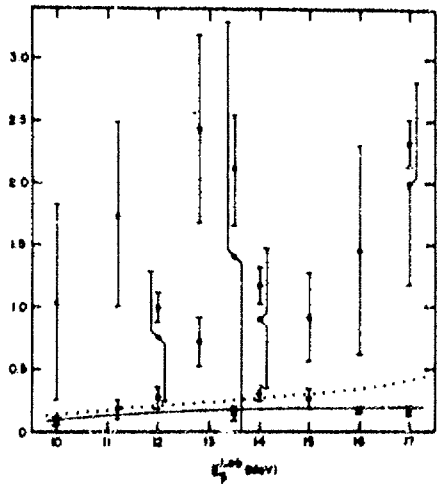

Figure 5. E2 cross sections for $^{12}C(\vec{p},\gamma_0)^{13}N$ (ref. 3). The solid points are determined from fitting all the a_i b_i, including secondary minima which satisfy a 1% confidence level. The open circles are determined from fits excluding a_1 and b_1. The curves are described in Fig. 4 caption.

Fitting all coefficients (solid points) gives at some energies two χ^2 minima for σ_{E2}. The higher σ_{E2} values correspond to large s/d E1 amplitude ratios that would be inconsistent with the smooth E1 behavior argued above. Small E2 solutions exist everywhere, roughly consistent with calculated direct E2 capture. Furthermore E1-direct E2 interference calculations using the DSD model correctly predict the general features of the a_i and b_i (Fig. 4). The open points in Fig. 5 result from an E2 analysis in which the a_i and b_i are excluded, the idea being to try to minimize first order effects from possible M1 contributions. This results in much bigger values and errors for σ_{E2}, at several energies in apparent disagreement with the lowest solid points. This analysis depends strongly on the tiny a_4 and b_4 coefficients, which are not well-determined experimentally. Hence these differences cannot be used as reliable indications of M1 radiation. Other studies show a similar pattern of results[5-7,13] indicating that the lowest solid points (lowest χ^2 minima for fitting all a_i b_i) represent estimated lower limits for σ_{E2} which are in fact our best estimates of the values of σ_{E2} if M1 can be neglected. Similar results are found for the E2 cross sections deduced in the $^{13}C(\vec{p},\gamma_1)^{14}N$ (ref. 13) and $^{14}C(\vec{p},\gamma_0)^{15}N$ (ref. 5) reactions (Fig. 6).

The E2 cross sections deduced from $^{15}N(\vec{p},\gamma_0)^{16}O$ measurements at Seattle are shown in Fig. 7 for E_p = 1.4 to 18.0 MeV (E_x = 13.4 to 29 MeV). The data include a reanalysis of the work of Bussoletti et al.,[6] plus new results[15] mainly at the lower energies. Aside from some small reso-

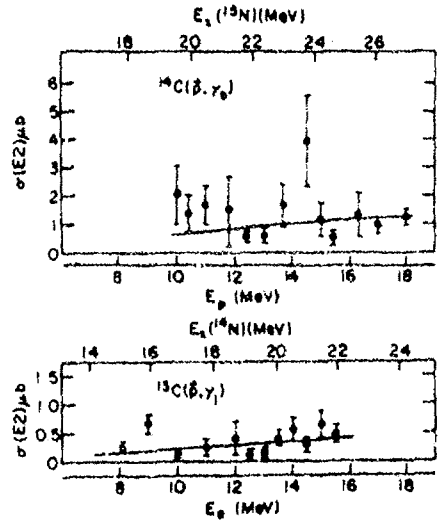

Figure 6. E2 cross sections for $^{13}C(\vec{p},\gamma_1)^{14}N$ (ref. 13) and $^{14}C(\vec{p},\gamma_0)^{15}N$ (ref. 5). The solid lines are calculated direct E2 capture.

nances below E_x = 20 MeV, the only region of possibly significant structure is for E_x = 23-27 MeV, where the present data indicate a strength of roughly 5-10% of the isoscalar E2 energy weighted sum rule (EWSR)[16] in excess of a smooth "background" estimated from the lower points in this region, in qualitative agreement with Stanford work.[2,18] For E_x = 17.9-27.3 MeV where $(\alpha,\alpha' p_0)$ coincidence decay studies[19]

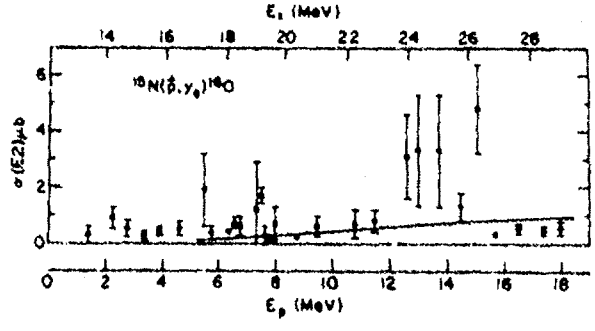

Figure 7. E2 cross sections for the $^{15}N(\vec{p},\gamma_0)^{16}O$ reactions (refs. 6, 15).

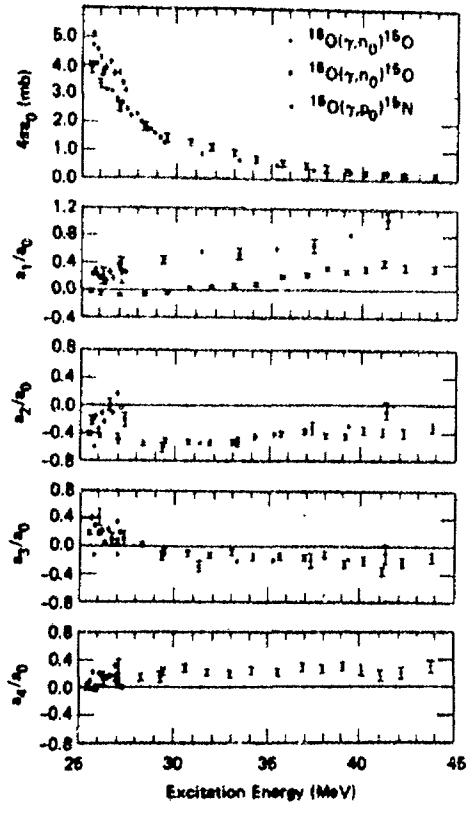

Figure 8. A comparison of $^{16}O(\gamma,n_0)$ and $^{16}O(\gamma,p_0)$ reactions (from ref. 19).

show 9% of the EWSR we find in (p,γ_0) 12-22% of the EWSR (calculated direct E2 capture accounts for ∿8% of the EWSR). Thus the integrated E2 strength seen in this region in $(\alpha,\alpha'p_0)$ and (p,γ_0) may be compatible when one accounts for direct capture, without the need to invoke the presence of significant isovector (IV) E2 strength. For E_x = 13.4 to 29 MeV (p,γ_0) shows 20-30% of the EWSR, with direct capture accounting for ∿11% of the EWSR.

The region above the GDR in ^{16}O has received special attention recently with new $^{16}O(\gamma,n_0)^{15}O$ results from Livermore.[19] Figure 8 shows a comparison of $^{16}O(\gamma,n_0)$ data[19,20] with $^{16}O(\gamma,p_0)^{15}N$ results derived from unpolarized radiative capture data.[21,22]

The odd a_1 and a_3 coefficients should be dominated by E1-E2 interference. A comparison of the values of a_1 and a_3 for p_0 and n_0 channels yields information on the isospin of the E2 (since the E1 is essentially pure IV). Pure IS or pure IV E2 would lead to comparable magnitudes for a_3 (and a_1) in p_0 compared with n_0, with the same signs for IV E2 and opposite signs for IS E2. The results clearly favor IV dominance, although some IS strength must also be present since the a_1's don't agree in magnitude. This may be partly due to direct E2 capture (which is an equal mixture of IS and IV).

The authors of ref. 19 have estimated a minimum E2 cross section $\sigma_{E2} > 0.875\ a_4\ \sigma_{total}$ (lower curve of Fig. 9) based only on the assumption that multipoles of higher order than E2 may be neglected. The corresponding lower-limit integrated E2 strength is 23% of the EWSR.[16] The large value for this lower limit results from the large measured a_4's (in contrast, (p,γ_0) shows small negative a_4's between 0.0 and -0.1 for E_x = 27-37 MeV). The importance of this result, along with the difficulty of the experiment, make an independent measurement highly desirable. The a_1 and a_3 coefficient alone in p_0 and n_0, as well as the a_4 observed in the p_0 channel are consistent with substantially smaller E2 cross sections.

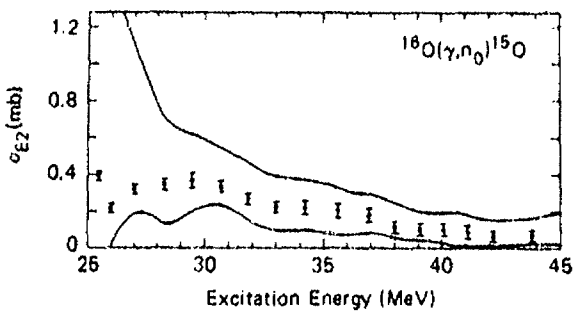

Figure 9. E2 cross section for $^{16}O(\gamma,n_0)$. The solid lines represent upper and lower limits, and the data points represent estimated values (from ref. 19).

V. M1 STRENGTH IN $(\vec{p},\gamma_0)$

Of particular interest is the recent discovery at Seattle[7,23] that M1 excitations can be uniquely identified in radiative capture. This has been done in the region of semi-isolated resonances below the GDR in the $^{15}N(\vec{p},\gamma_0)^{16}O$ reaction, as illustrated in Fig. 10. Here the χ^2 for fitting angular distributions assuming only E1 and E2 radiation is plotted versus energy, along with other observables. Strong deviations from acceptable values ($\chi^2 \lesssim 2$) indicate areas

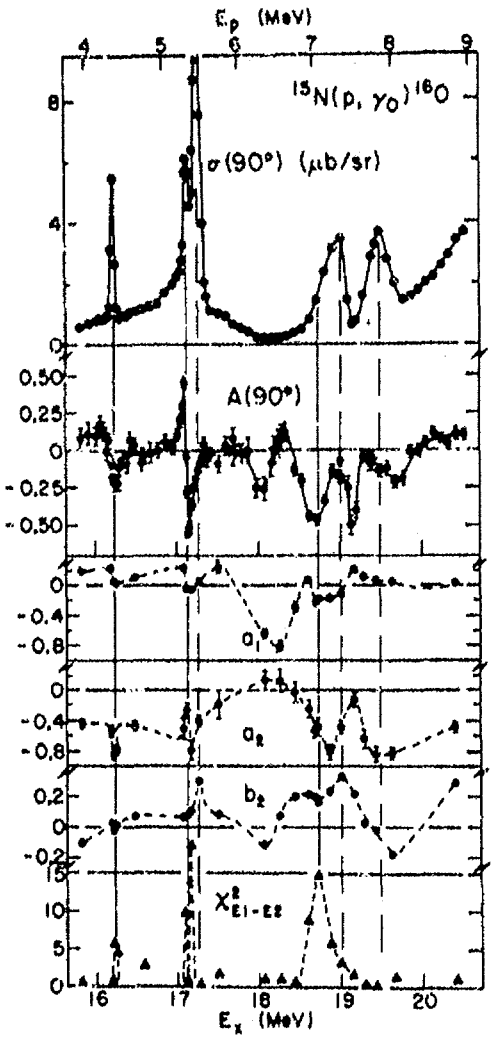

Figure 10. Excitation curves for $^{15}N(\vec{p},\gamma_0)^{16}O$: $\sigma(90°)$, $A(90°)$ and the a_1, a_2 and b_2 coefficients (3rd and 4th order coefficients not shown) and the reduced χ^2 for angular distribution fits assuming only E1 and E2 radiation. The curves are to guide the eye. Vertical solid and dashed line lines indicate M1 and E1 resonances, respectively (ref. 23).

of concentrated M1 strength. Analysis of the a_i and b_i near these energies shows that the prominent resonances at 16.22 and 17.14 MeV are M1, with a third M1 resonance near 18.8 MeV which in the cross section is unresolved from a neighboring E1 resonance.

These M1 resonances in ^{16}O correspond to a total ground-state M1 strength $B(M1)\uparrow \gtrsim 0.24\ \mu_0^2$. This is quite sizable compared to a non-closed shell A = 4n nucleus such as $^{12}C(B(M1)\uparrow = 0.93\ \mu_0^2)$, when one recalls that such strength is "forbidden" since the doubly-magic closed shell cannot contribute to M1 excitations. The observed M1 decays stem from the ground-state correlations (primarily 2 particle-2 hole) and are in reasonable accord with recent shell model calculations.[24] Very recently, electron scattering has been

used to search for similar transitions in ^{40}Ca, with a definitive M1 assignment for a strong ($B(M1)\uparrow = 0.37\ \mu_0^2$) transition at 10.32 MeV.[25] It is interesting to note that this one state in ^{40}Ca carries more M1 strength than the total of all the known M1 strength in ^{16}O. These results are summarized in Fig. 11.

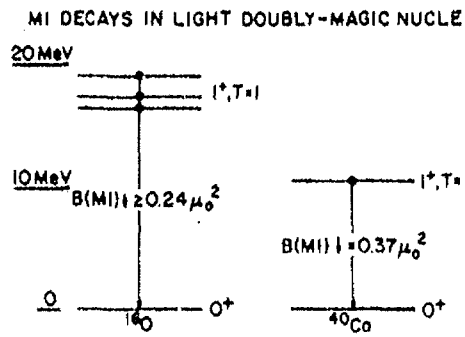

Figure 11. Summary of known ground state M1 decays in the doubly-magic ^{16}O and ^{40}Ca nuclei.

The ability of $(\vec{p},\gamma)$ for discovering M1 transitions has so far been demonstrated only in the one case discussed above. In the future it will be interesting to extend this technique to other nuclei, and to see if M1 resonances can be identified in reactions which do not have the simplest spin sequences.

VI. ALPHA CAPTURE

The experimental technique of radiative α-capture is particularly straightforward. For capture on a spin-zero target leading to a spin-zero residual state (of the same parity) only electric multipoles may contribute (in practice E3 and higher multipoles may usually be neglected), and from the angular distribution one can uniquely separate E1 and E2.

$$\sigma(E,\theta) = \frac{3}{8\pi}\sigma_{E1}(E)\sin^2\theta + \frac{15}{32\pi}\sigma_{E2}(E)\sin^2 2\theta + \frac{3}{8\pi}[5\sigma_{E1}(E)\,\sigma_{E2}(E)]^{1/2}\sin\theta\sin 2\theta\cos\phi(E)$$

where $\phi(E)$ is the E1-E2 relative phase. The above equation is appropriate for a point geometry—finite geometry effects are usually accounted for by expressing the above in terms of Legendre polynomials $P_k(\cos\theta)$ and replacing P_k by $Q_k P_k$.

The systematics of α capture are reasonably well-established (see ref. 26 for many of the relevant experimental references). E1 capture is generally dominated by compound processes—that this should be true for isospin allowed ($T_z(\text{target}) \neq 0$) as well as for isospin forbidden

cases follows from the smallness of the kinematic E1 effective charge; i.e., the α-nucleus interaction is essentially pure isoscalar and hence cannot excite the isovector doorway GDR. Since E1 capture is compound, the interference term above averages to zero in cases where the compound levels are sufficiently dense. The α_0 channel, except in special cases in light nuclei, is not a strong decay mode of the IS GQR[27] and $\sigma_{E2}(\alpha,\gamma)$ does not generally show the GQR gross structure envelope (in contrast to E1 radiation in the (p,γ) reaction which does show the GDR gross structure envelope). This is, apparently, because $\sigma_{E2}(\alpha,\gamma)$ is dominated by compound decay. The dominance of compound decay explains the peaking of $\sigma_{E2}(\alpha,\gamma)$ below the main GQR in light nuclei (for $A \sim 58$, $\sigma_{E2}(\alpha,\gamma)$[26] and the GQR strength function[27] have similar shapes due to the accidental proximity of the GQR to the α-nucleus Coulomb barrier). However, statistical decay calculations using the GQR strength function deduced from (α,α') experiments generally fall short of reproducing the observed (α,γ) cross sections, indicating some pre-equilibrium contribution in this reaction. This makes it difficult to determine the GQR strength function from $\sigma_{E2}(\alpha,\gamma)$ data. On the other hand, such data has proven very useful in mapping the fragmentation of E2 strength below the GQR in light nuclei.

The gross properties of the IS GQR are now well-established, primarily from α-scattering experiments (see ref. 27). It is ironical, perhaps, that in such experiments the electromagnetic (EM) interaction does not play an important role, but rather it is from the strong (nuclear) interaction that one infers how the nucleus would respond to E2 photons at giant resonance energies. However, E2 strength inferred from decay coincidence $A(\alpha,\alpha'\alpha_0)B$ experiments may be directly compared with E2 strength observed in $B(\alpha,\gamma_0)A$ reactions. ^{16}O is currently the 'best case for such a comparison. Here, low-lying (E_x < 12 MeV) electromagnetic strength agrees fairly well with (α,α') strength[28] but in the "GQR" region (E_x = 17.9-27.3 MeV) the $(\alpha,\alpha'\alpha_0)$ E2 strength[17] is more than a factor of 2 greater than (α,γ_0) E2 strength[29] (13% of the EWSR compared to 5%, respectively). For E_x = 19.2 to 27.3 MeV (this excludes the resonance just above 18 MeV), $(\alpha,\alpha'\alpha_0)$ shows 10% of the EWSR, and (α,γ_0) only 2.5% of the EWSR. Isospin mixing has been cited as a plausible explanation for these differences, but the magnitude required is substantial. For mixing of IS and IV (isovector) excitations of comparable intrinsic strength, one must have a relative T = 1 to T = 0 amplitude impurity[27] in the IS GQR of $\beta_1/\beta_0 \sim 0.3$-0.5 (where $(1 + \beta_1/\beta_0)^{-2} = 2$-$4$) to explain a factor of 2-4 in the $(\alpha,\alpha'\alpha_0)/(\alpha,\gamma_0)$ strength ratio.

Since a strong T-mixing matrix element is $\lesssim$ 0.15 MeV,[30] this requires energy denominators of order 0.5-0.3 MeV for 2-state mixing, which is unreasonably small if one takes resonance widths as well as energies into account. If many levels are involved, then one would expect substantial variation in T-mixing over energy intervals of this magnitude. However, the close similarity of the structure in these reactions over the much wider GQR range (18-27 MeV) (see Fig. 3 of ref. 17) makes it unlikely that this is happening. I feel that these strength differences are yet to be explained satisfactorily.

VII. NEUTRON CAPTURE

The TUNL group[31] is rapidly pushing back the technological frontier in the area of neutron capture. The latest qualitative advance in technique is described in ref. 31 where results of impressive quality are presented for the $^{40}Ca(\vec{n},\gamma_0)$ reaction at E_n = 10 MeV, in the region of the IS GQR (see Fig. 12). These results show definite evidence for

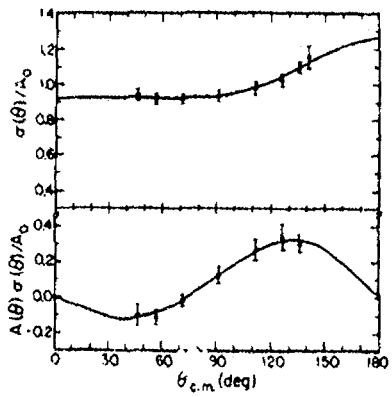

Figure 12. The $^{40}Ca(\vec{n},\gamma_0)^{41}Ca$ reaction at E_n = 10.0 MeV (from ref. 31).

non-zero E2 (M1) radiation, with b_1 = 0.13 ± 0.02; however, it will take additional energy points to reveal whether these effects come from the GQR. It is interesting in this context to note that in $(\vec{p},\gamma)$ into ^{16}O, for example, the b_1 coefficients are much larger below the main IS GQR region, where relatively narrow E2 and M1 resonances occur.

VIII. GIANT RESONANCES BUILT ON HIGHLY EXCITED STATES

One of the very interesting areas of research currently accessible only through the technique of radiative capture is the study of giant resonances built on excited nuclear

states. Recent work by Blatt and co-workers[32] has revealed strong radiative proton capture transitions from the continuum to highly excited residual states at bombarding energies of 40-100 MeV in several light nuclei. These highly excited residual states are themselves unbound, so that the "capture" process is really a "nuclear bremsstrahlung" (p,γx) reaction where x represents the (unobserved) particles emitted following the γ-ray. Identification of this process was made from the experimental observation of the proper kinematical relation between E_γ and E_p.

Figure 13, taken from the discussion of Arnold,[33] displays spectra from the $^{11}B(p,\gamma)$ and $^{12}C(p,\gamma)$ reactions[32] at E_p = 40 MeV. The $^{11}B(p,\gamma)$ reaction at this energy strongly populates a group of states near 19 MeV excitation energy. The spectrum shape is in qualitative accord with the solid vertical lines which represent the shell-model $1\hbar\omega$ particle-hole spectrum for $16 \lesssim E_x \lesssim 25$ MeV, consisting mainly of $[(1p_{3/2})^{-1}(2s,1d)^1](J^\pi = 0^- \ldots 4^-)$ configurations, with the high spin states expected to dominate.

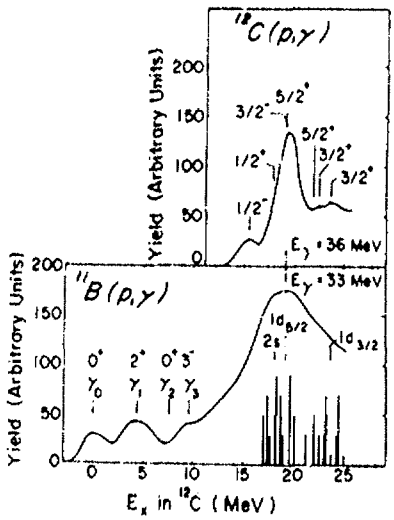

Figure 13. Solid curves: Spectra from $^{11}B(p,\gamma)$ and $^{12}C(p,\gamma)$ at E_p = 40 MeV ($r^{12}C(p,\gamma)$ at E^e solid vertical lines represent the shell model $1\hbar\omega$ par. le-hole spectrum for E_λ 16-25 MeV in ^{12}C (from ref. 33).

The $^{12}C(p,\gamma)$ spectrum at a similar γ-ray energy should show a roughly similar shape, corresponding to the low-lying single particle sd-strength distribution in ^{13}N, as appears to be the case (Fig. 13). Simple considerations lead one to expect a giant E1 resonance built on every excited state, with a strength in (p,γ) related to the stripping spectroscopic factor connecting the target and the excited (final) state (in the DSD model, such a spectroscopic factor enters explicitly). For example, the magnitudes of the $^{11}B(p,\gamma)$ and $^{12}C(p,\gamma)$ reactions for similar γ-ray energy should be equal if one sums over final states which contain the same

single-particle stripping strength.

Weak-coupling arguments would say that the expected GDR energy is just the ground-state GDR energy plus the excitation energy of the final state, or $E_x \approx 19 + 23 = 42$ MeV ($E_p = 28$ MeV) for the $^{11}B(p,\gamma)$ example above, as appears to be the case experimentally.[34] Thus it is quite possible that one is seeing "$2\hbar\omega$ giant resonances"; i.e., $1\hbar\omega$ giant E1 resonances built on the $1\hbar\omega$ final states. However, it might be possible that a simple direct capture mechanism could explain the results. For final states below 10 MeV in ^{12}C, "giant" resonances are observed in the $^{11}B(p,\gamma)$ reaction,[35] with properties in rough accord with the above discussion.

IX. DECAY OF HIGH SPIN PARTICLE-HOLE STATES

Narrow "stretched" high spin particle hole states are found in nuclei from ^{12}C to ^{208}Pb and have been studied in high energy electron, proton, and pion scattering and in some cases in direct transfer reactions. The lowest T = 1 levels of this sort such as $[d_{5/2},p_{3/2}^{-1}](4^-1)$ in ^{12}C and ^{16}O (refs. 36,37) and $[f_{7/2},d_{5/2}^{-1}](6^-1)$ in ^{24}Mg and ^{28}Si (see ref. 38) are believed to be predominantly 1 particle-1 hole states, which is part of the reason why they are so interesting. In ^{16}O, for example, the 4^-,1 state at 18.98 MeV has nearly all of the expected (d,t) pickup strength,[39] and has $\sim 1/2$ of the M4 "single particle" inelastic electron scattering strength.[38] The excitation of these levels is the subject of a separate paper by Lindgren at this conference—what I'd like to do here is to briefly discuss the γ-decay of these states, which can provide valuable structure information complementary to the excitation experiments.

Figure 14 shows some old Oxford data[40] for the $^{15}N(p,\gamma_{1,2})^{16}O$ reaction populating the 0^+, 3^- doublet at 6.1 MeV. Of particular interest are the resonances at $E_x \approx 18$ and 19 MeV) which correspond to the γ-decays of the 3^-, T = 1 (18.03 MeV) and 4^-, 1 (18.98 MeV) levels, respectively, to the 3^-, 0 (6.13 MeV) level. These assignments are based primarily on recent Seattle measurements[41] of $^{15}N(p,\gamma_{1,2})$, $(p,\alpha_1\gamma)$ and $(p,p_{1,2,3}\gamma)$ which show agreement in excitation energy and in the dominant particle decay channel with the Heidelberg data.[42] The angular distributions for these resonances are consistent with pure M1 decay.[40] Combining the resonance strengths of ref. 40 with the p_0 branching ratios of ref. 42 ($\Gamma_{p0}/\Gamma = 0.41 \pm (0.10\text{-}0.20)$ and 0.12 ± 0.05 for the $(3^-,1)$ and $(4^-,1)$ levels, respectively) gives rough decay strengths B(M1) ~ 0.1 W.U. and ~0.2 W.U.[43]

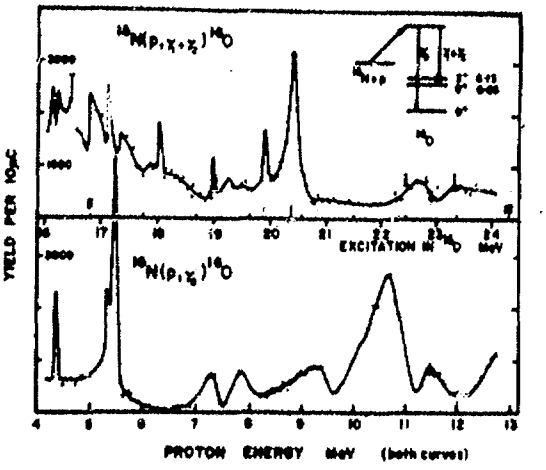

Figure 14. 90° yield curve for the $^{15}N(p,\gamma_0)$ and the $^{15}N(p,\gamma_{1,2})^{16}O$ reactions (from ref. 40).

for the $(3^-,1) \rightarrow (3^-,0)$ and the $(4^-,1) \rightarrow (3^-,0)$ decays, respectively. The $(4^-,1) \rightarrow (3^-,0)$ decay strength is in accord with the shell model value of 0.23 W.U. calculated[44] by J. Millener (using a $1\hbar\omega$ basis), but is not accurate enough to serve as a real test of the 1p-1h purity of the $(4^-,1)$ level. Such a test must await improved strength measurements which are in progress at Seattle.[41] The reasonably strong $(3^-,1) \rightarrow (3^-,0)$ decay strength is also interesting since this level is not particularly strong in pickup,[39] implying it should be mostly 3p-3h.

As a final comment, I would like to point out the one other case where a γ-decay is known for a stretched high spin particle-hole state. In ^{28}Si the $[f_{7/2},d_{5/2}^{-1}](6^-,1)$ level at 14.36 MeV has a γ-branch[45] of 100% to the $(6^-,0)$ "antianalog" state at 11.58 MeV, with B(M1) = 0.7 ± 0.15 W.U. (assuming $\Gamma_p >> \Gamma_\gamma$). This is considerably weaker than the calculated[44] analog-antianalog decay strength of 8 W.U. for pure $[f_{7/2},d_{5/2}^{-1}](6^-)$ configurations, perhaps due to fragmentation of the antianalog configuration.

Clearly the decay spectroscopy of these stretched particle-hole states is still in its infancy, and should lead in the future to a great deal of useful information regarding the structure of these unusual states.

X. CONCLUSIONS

I hope I leave you with the impression that there is a lot of new and exciting work going on in radiative capture studies. Besides the new directions that I've indicated in my discussion above, I would like to comment specifically on 2 additional areas that one should watch for future developments. One, which I've barely mentioned at all (since this

was by design mainly an experimental talk) is the theoretical development of radiative capture calculations. In particular one may hope that the work of Dietrich and Kerman[46] will lead to a predictive capture theory. The value of such a theory is obvious when one recalls the wide variety of experimental data on E1-E2 interference effects in (p,γ) and (n,γ) which I've hardly touched upon, which might be understood with an improved theory. The second area is the field of polarized proton capture, where essentially all experiments to date of which I'm aware have been limited by source intensity. The new generation of high intensity polarized negative hydrogen ion sources will permit qualitative advances in $(\vec{p},\gamma)$ studies in the resonance region.

ACKNOWLEDGEMENTS

I am indebted to my colleagues who have shared in experiments performed in Seattle in the past few years, including E.G. Adelberger, J.E. Bussoletti, K. Ebisawa, P.G. Ikossi, K.T. Lesko, and T.A. Trainor.

This work has been supported by the United States Department of Energy.

REFERENCES

1. H.F. Glavish, S.S. Hanna, R. Avida, R.N. Boyd, C.C. Chang, and E. Diener, Phys. Rev. Lett. 28, 766 (1972).
2. S.S. Hanna, H.F. Glavish, R. Avida, J.R. Calarco, E. Kuhlman, and R. LaCanna, Phys. Rev. Lett. 32, 114 (1974).
3. R. Helmer, M.D. Hasinoff, J.E. Bussoletti, K.A. Snover, and T.A. Trainor, submitted to Nucl. Phys.
4. D. Berghofer, M.D. Hasinoff, R. Helmer, S.T. Lim, D.F. Measday, and K. Ebisawa, Nucl. Phys. A263, 109 (1976).
5. K.A. Snover, J.E. Bussoletti, K. Ebisawa, T.A. Trainor, and A.B. McDonald, Phys. Rev. Lett. 37, 273 (1976).
6. J.E. Bussoletti, Ph.D. Thesis, University of Washington, 1978; K.A. Snover, J.E. Bussoletti *et al.*, to be published.
7. K.A. Snover, Proc. of the 3rd Internat. Symp. on Neutron Capture Gamma Ray Spectroscopy and Related Topics, Brookhaven, 1978 (Plenum Press, NY), p. 319.
8. D.G. Mavis, H.F. Glavish, and D.C. Slater, Proc. of the 4th Internat. Symp. on Polarization Phenomena in Nuclear Reactions, Zurich, 1975 (Birkhäuser Press, Basel), p. 749.
9. D.H. Wilkinson, Physica 22, 1039 (1956).

10. K.A. Snover, P.G. Ikossi, E.G. Adelberger, and K.T. Lesko, to be published.
11. P.E. Marrs, E.G. Adelberger, and K.A. Snover, Phys. Rev. C 16, 61 (1977).
12. J.R. Calarco, S.W. Wissink, M. Sasao, K. Wienhard, and S.S. Hanna, Phys. Rev. Lett. 39, 925 (1977).
13. J.D. Turner, N.R. Robertson, S.A. Wender, H.R. Weller, and D.R. Tilley, submitted to Phys. Rev. C.
14. D.G. Mavis, Ph.D. thesis, Stanford University, 1977, unpublished.
15. K.A. Snover, P.G. Ikossi, and K.T. Lesko, to be published.
16. M. Gell-Mann and V.L. Telegdi, Phys. Rev. 91, 169 (1953). We use values for $\langle r^2 \rangle$ taken from electron scattering: C.W. de Jager *et al.*, Atomic and Nuclear Data Tables 14, 479 (1974).
17. K.T. Knöpfle, G.J. Wagner, P. Paul, H. Breuer, C. Mayer-Böricke, M. Rogge, and P. Turek, Phys. Lett. 74B, 191 (1978).
18. S.S. Hanna, Proc. of the Internat. Conf. on Nuclear Physics with Electromagnetic Interactions, Mainz, Germany, June 1979. Lecture Notes in Physics 108, 288 (1979).
19. T.W. Phillips, and R.J. Johnson, Phys. Rev. C, to be published.
20. J.W. Jury, J.S. Hewitt, and K.G. McNeil, Can. J. Phys. 48, 1635 (1970).
21. P. Paul, J.W. Noé, K.A. Snover, M. Suffert, E.K. Warburton, and H.M. Kuan, Proc. of the Internat. Symp. on Highly Excited States in Nuclei, Julich, 1975, Vol. 1, p. 2.
22. W.J. O'Connell, and S.S. Hanna, Phys. Rev. C 17, 892 (1978).
23. K.A. Snover, P.G. Ikossi, and T.A. Trainor, Phys. Rev. Lett. 43, 117 (1979).
24. A. Arima and D. Strottman, Phys. Lett., to be published.
25. W. Gross, D. Meuer, A. Richter, E. Spamer, O. Titze, and W. Knüpfer, Phys. Lett. 84B, 296 (1979).
26. L. Meyer-Schutzmeister, R.E. Segel, K. Raghunathan, P.T. Debevec, W.R. Wharton, L.L. Rutledge, and T.R. Ophel, Phys. Rev. C 17, 56 (1978).
27. K.T. Knöpfle, Proc. of the Internat. Conf. on Nuclear Physics with Electromagnetic Interactions, Mainz, Germany, June 1979; Lecture Notes in Physics 108, 311 (1979).
28. K.T. Knöpfle, G.J. Wagner, H. Breuer, M. Rogge, and C. Mayer-Böricke, Phys. Rev. Lett. 35, 779 (1975).
29. K.A. Snover, E.G. Adelberger, and D.R. Brown, Phys. Rev. Lett. 321, 1061 (1974).

30. E.G. Adelberger, R.E. Marrs, K.A. Snover, and J.E. Bussoletti, Phys. Rev. C 15, 484 (1977).
31. M. Jensen, D.R. Tilley, H.R. Weller, N.R. Robertson, S.A. Wender, and T.B. Clegg, Phys. Rev. Lett. 43, 609 (1979).
32. M.A. Kovash, S.L. Blatt, R.N. Boyd, T.R. Donoghue, H.J. Hausman, and A.D. Bacher, Phys. Rev. Lett. 42, 700 (1979).
33. L.G. Arnold, Phys. Rev. Lett. 42, 1253 (1979).
34. S.L. Blatt, M.A. Kovash, H.J. Hausman, T.R. Donoghue, R.N. Boyd, A.D. Bacher, and C.C. Foster, contributed paper to this conference.
35. K.A. Snover, P. Paul, and H.M. Kuan, Nucl. Phys. A285, 189 (1977).
36. T.W. Donnelly, J.D. Walecka, I. Sick, and E.B. Hughes, Phys. Rev. Lett. 21, 1196 (1968).
37. I. Sick, E.B. Hughes, T.W. Donnelly, J.D. Walecka, and G.E. Walker, Phys. Rev. Letts. 23, 1117 (1969).
38. R.A. Lindgren, W.J. Gerace, A.D. Bacher, W.G. Love, and F. Petrovitch, Phys. Rev. Lett. 42, 1524 (1979) and references therein.
39. G. Mairle, G.J. Wagner, P. Doll, K.T. Knöpfle, and H. Breuer, Nucl. Phys. A299, 39 (1978).
40. A.R. Barnett and N.W. Tanner, Nucl. Phys. A152, 257 (1970). See also S.H. Chew, J. Lowe, J.M. Nelson, and A.R. Barnett, Nucl. Phys. A229, 241 (1974); Nucl. Phys. A286, 451 (1977).
41. K.A. Snover, P.G. Ikossi, E.G. Adelberger, and K.T. Lesko, to be published.
42. H. Breuer, P. Doll, K.T. Knöpfle, G. Mairle, and G.J. Wagner, preprint.
43. One Weisskopf Unit (W.U.) = 1.79 $\mu\beta$.
44. J. Millener, private communication.
45. G.F. Neal and S.T. Lam, Phys. Lett. 45B, 127 (1973).
46. F.S. Dietrich and A.K. Kerman, Phys. Rev. Lett. 43, 114 (1979).